Journal of Power Sources 247 (2014) 332–338

Contents lists available at ScienceDirect

Journal of Power Sources

journal homepage: www.elsevier.com/locate/jpowsour

Production caused variation in capacity aging trend and correlation to initial cell performance

Thorsten Baumhöfer [a, c, *], Manuel Brühl [a], Susanne Rothgang [a, c], Dirk Uwe Sauer [a, b, c]

[a] Electrochemical Energy Conversion and Storage Systems Group, Institute for Power Electronics and Electrical Drives (ISEA), RWTH Aachen University, Aachen, Germany
[b] Institute for Power Generation and Storage Systems (PGS), E.ON ERC, RWTH Aachen University, Germany
[c] Jülich Aachen Research Alliance, JARA-Energy, Germany

HIGHLIGHTS

- Aging of equal cells under equal conditions results in significant lifetime differences.
- An experiment with consideration of uncertainties validates this assumption.
- Aging trend differences lead to less than optimal lifetime of battery packs.
- Attributes from initial performance tests can be used to classify the cells.

ARTICLE INFO

Article history:
Received 24 June 2013
Received in revised form
20 August 2013
Accepted 27 August 2013
Available online 5 September 2013

Keywords:
Lithium-ion
Cell-to-cell variation
Aging variance
Aging prediction
Data mining

ABSTRACT

Battery packs usually consist of multiple individual cells in a series connection, thus the worst cell defines the pack's performance. All cells do age individually causing a spread in cell performance. We will show that not only the local operating conditions, but also variances from within the cell manufacturing process influence the variation of aging trends. By an experiment with 48 cells from a mass production line it can be found that the aging spread cannot be neglected. Using data mining algorithms a dependency between initial cell performance and cycle lifetime is identified. The resulting linear regression model can predict the lifetime and can therefore be used to classify cells into different batches before battery pack production.

1. Introduction

Lithium-ion batteries are spreading into more and more fields of application. Starting with consumer electronics products in the 1990s, they also dominate the market for power tool and electric bike batteries, lately. But with the application in hybrid and full electric vehicles the requirements changed. A vehicle has an average lifespan of ten to fifteen years compared to an average lifespan of three to five years in the other fields of application. Thus the battery aging has to be considered in much greater detail.

A battery pack in electric vehicles usually consists of around hundred battery cells in a series connection. Ideally all these cells are exactly equal. But as these cells are electrochemical systems, they possess sheer endless possibilities for variance. From the base materials (such as grain size distribution of the active materials) over process parameters during fabrication (such as the film thicknesses or drying times) up to the formation procedure and storage times everything contributes to uncertainties in the cells characteristics. Modern process control and quality assurance techniques can help to reduce the uncertainties, but due to the complex dependencies some uncertainties will remain. Santhanagopalan and White [1] address this by using a physio-chemical model to identify sensitivities of the initial cell impedance on different fabrication parameters. But it is obviously impossible to directly measure the variances in aging behavior for quality control.

Looking at the aging prediction, different battery aging mechanisms were identified and it was shown that these are highly

* Corresponding author. Electrochemical Energy Conversion and Storage Systems Group, Institute for Power Electronics and Electrical Drives (ISEA), RWTH Aachen University, Aachen, Germany.
E-mail addresses: batteries@isea.rwth-aachen.de, tba@isea.rwth-aachen.de (T. Baumhöfer).
URL: http://www.isea.rwth-aachen.de

0378-7753/$ – see front matter © 2013 Elsevier B.V. All rights reserved.
http://dx.doi.org/10.1016/j.jpowsour.2013.08.108

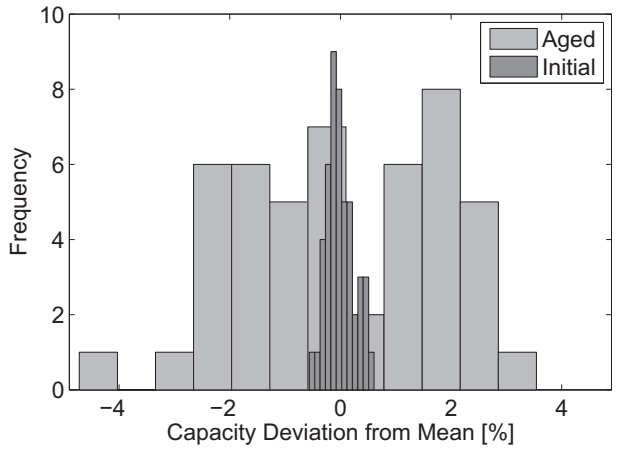

Fig. 1. The deviations between the capacities from 48 new and equally aged cells (relative to their mean capacity) do widen during aging, even under the same conditions.

dependent on the used chemistry, design parameters and battery usage [2]. This indicates that there is the need to conduct aging experiments for a specific application with the cell selected for this application. Only with experiments it is possible to quantify the influence of the different aging phenomena and to parameterize empirical aging models [3]. The different operating condition parameter like temperature, range of state of charge (SoC) and applied current define the need for not only one aging test point but a whole matrix. Since aging tests have a long duration and every measurement channel costs a substantial amount of money, tests cannot be conducted for all possible combinations. The selection of test points is either done by expert knowledge [4–6] or by conducting a design of experiment [7]. Due to the same cost limitations usually a maximum of three cells are tested in one test point. This allows detecting outliers, but has no statistical significance in quantifying the variance within the aging trends. Dubarry et al. [8] state that a low initial variance of cell parameters (capacity, polarization resistance, delivery SoC) does also result in a low variation of the aging trends. Due to the equality these cells could therefore be used in aging test matrices. Even though the tendency is certainly true one can see in Fig. 1, that a variance in aging trend is existing (for the Experimental setup see Section 2). Thomas et al. [9] did also measure three cells per test point, but use an error model and Monte Carlo simulations to calculate confidence intervals for the aging trends.

Considering the variance is mandatory, because different aging trends have a large influence on battery pack performance. The weakest cell defines the performance in a series connection of cells. Dubarry et al. [10] showed that even the initial variance has to be considered by testing 100 cells and incorporating the variance in a battery pack model. A model considering a variance parameter complies with the pack's measurement results more accurately. This is valid for the differences in aging trend as well. Also the different temperatures at different positions in the battery pack have to be considered. Paul et al. [11] showed with Monte Carlo simulations that the battery pack design has a large influence on the dispersion in aging trends and Lih et al. [12] showed that there are indeed capacity differences in battery packs used in field tests.

In this work results from an aging test at one test-point but with a large sample base are shown. A cyclic aging profile was used and only the capacity degradation is examined. The results are a first indication of how large differences in aging can be. It is investigated if there are correlations between the initial performance and the aging trend. Such a correlation would help the cell manufacturer with quality control or allow battery pack manufactures to sort cells prior to pack production in classes of different predicted aging behavior.

2. Experimental setup

In the experiment 48 cells of the same type were aged with the same profile under equal conditions. Prior to aging the initial performance was determined by a comprehensive begin-of-life (BOL) test. Aging reference parameter tests (RPT) were conducted in regular intervals to determine the current cell performance. Due to measurement equipment limitations the tests were started with batches of four cells every two to three days and thus slightly shifted in time.

Cells. The cells used in this investigation are Sanyo/Pana-sonic UR18650E cylindrical cells which are commercially available and produced in large quantities in an established fabrication process. This type uses a carbon anode and NMC as a cathode material. These cells were graded into group C from the manufacturer and are drawn from the same production lot. Due to this factory selection the cells only have a mean capacity of approximately 1.85 Ah compared to the A-grade nominal capacity of 2.05 Ah.

Procedures. The first part of the begin-of-life test is a measurement of pulse resistances without prior conditioning of the cell. All cells are delivered at nearly the same state of charge, which is set by the manufacturer after formation to minimize aging during storage. An optimal procedure for cell selection would work at this SoC to save the time for conditioning the cell. Thus only temperature equalization to 25 °C is performed before the pulse resistance test at the delivery SoC. Next the capacity for different current rates is being determined. The cut-off voltage and maximum charge voltage are chosen to be moderate (3 V and 4.1 V) to minimize the stress from BOL and RPT testing. The charging is conducted with constant current of 2 A and the maximum charge voltage is being held until the current is lower than 40 mA. The pulse resistances followed by an impedance spectrum are measured at three different temperatures and three different voltage levels. To set the voltage level the cell is first charged and then discharged using a constant current of 2 A until the desired voltage is being reached. Then this voltage is held until the current is lower than 40 mA. This conditioning is always performed at 25 °C, afterward the measurement temperature is set. The three voltage levels (see Table 1) correspond to approximately 70%, 50% and 30% state of charge.

Cycling of the cells is conducted at a constant ambient temperature of 25 °C. One cycle consists of 30 min discharging to 3.5 V and 30 min charging to 3.9 V, both current limited to a maximum of 4 A. The charge turnover is about 1 Ah and corresponds to cycles

Table 1
Attributes at different operating conditions considered for the dependency analysis.

Measured Attribute	Temperatures	Current rates	Voltage level	Timepoint
Delivery State Of Charge	25 °C	2 A	–	–
Capacity	25 °C	2 A/1 A/0.5 A	–	–
Pulse Resistance	0 °C/25 °C/50 °C	±6 A/±4 A/±2 A	Delivered/3.85 V/3.7 V/3.6 V	0.4 s/1 s/2 s/5 s/10 s/15 s/20 s
Impedance	0 °C/25 °C/50 °C	0 A	3.85 V/3.7 V/3.6 V	See Fig. 3

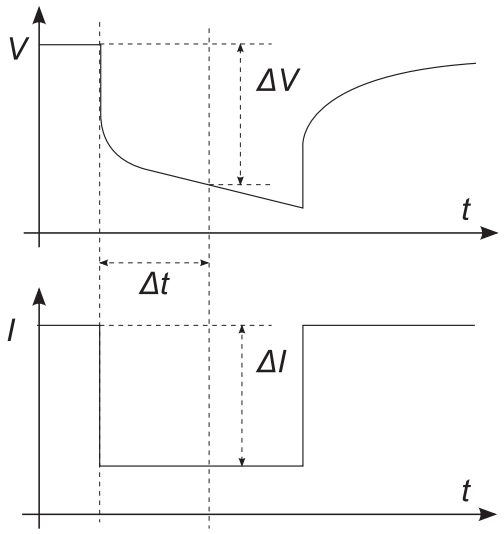

Fig. 2. Pulse resistance defined as the relation of voltage drop to current pulse amplitude at a specific timepoint.

between approximately 20% and 80% state of charge. Because of the voltage limits the charge turnover varies with the state of health of the cell, but the depth of discharge in relation to the aged capacity is being kept nearly constant (only influenced by the resistance increase). This cycling methodology is motivated by real world applications where the operating regime is limited by the voltage levels and also helps to reduce the influence of the test equipment variations.

The RPT only includes the capacity tests and pulse resistance tests at 25 °C but at all three voltage levels. No impedance measurements are included. In this work only the 2 A discharge capacity is being used as the performance measure.

Considered attributes. Different attributes are being determined from the conducted BOL test and are used to identify correlations subsequently. The discharged capacity for the three different currents is considered together with the mean temperature during the discharge. From the charge and discharge pulses with different currents, pulse resistances ($R_p = \Delta V/\Delta I$) are calculated for different timepoints Δt, specified from the beginning of the current pulse (see Fig. 2 and Table 1). Likewise the temperature at the different timepoints is considered. From the impedance spectrum the frequency, real and imaginary part of the impedance are considered in three characteristic points: The zero-crossing which indicates the pure ohmic impedance. The top point of the first semicircle, which

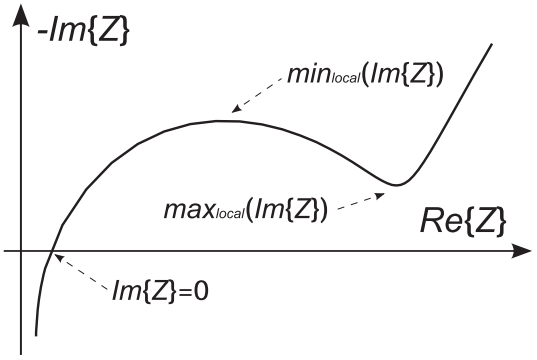

Fig. 3. Characteristic points in the impedance spectrum (note the reversed imaginary axis).

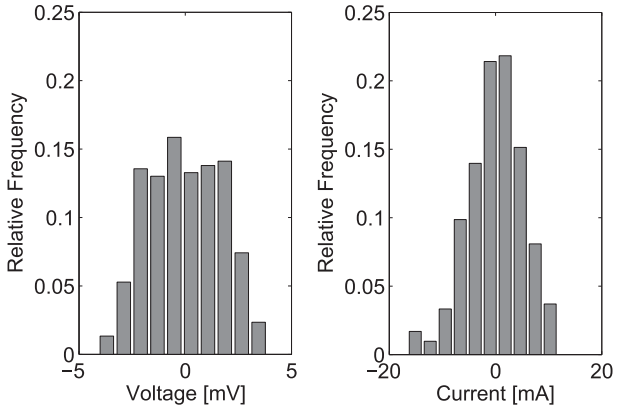

Fig. 4. Deviations within the measured voltage and set current of all used circuits during the verification measurement.

is defined by the local minimum of the imaginary part of the impedance. And the turning point after the semicircle, which is defined by the local maximum (see Fig. 3). Overall there are more than 950 individual attributes for each cell.

Equipment. The cycling was done on individual electrical circuits of a Digatron MCFT battery tester. All cells were stored within one Binder MK 720 temperature chamber. Each cell was mounted on an individual holder to allow good air flow and minimize the influence of neighboring cells. A temperature sensor (Dallas Semiconductor DS18B20) was glued to the middle of each cells steel housing.

To be able to assess the variation in aging trends it is important to quantify the variation of the different circuits and determine their influence on the experiment. To ensure the values given in the datasheets a verification measurement was conducted. Each circuit was sequentially connected to a Burster Digistant 4462 voltage reference and an Agilent 34401A multimeter. The circuit was set to provide a constant current and measure the voltage. About 60 measurement values were acquired during 1 min for each channel. Histograms from the deviations between all measurement values of all 48 circuits can be found in Fig. 4. All values show better parameters than stated in the manufacturer's specifications due to a recent calibration. The standard uncertainties according to the "Guide to the expression of uncertainty in measurement" [13] are given in Table 2. The column "between channels" describes the variation within all 48 channels; the column "within channel" gives the maximum uncertainty caused by noise considering one channel at a time. The values for the temperature sensors and impedance measurement are derived from datasheet values. Since the derived values for capacity and pulse resistance depend on the current and/or voltage operating point only the maximum uncertainty is given.

Due to the open circuit voltage slope the influence of the voltage uncertainties during cycling can only result in 0.17% variation of the SoC range. The current uncertainty has no great influence since the cycling is not based on coulomb counting and therefore error

Table 2
Standard uncertainties for the measurement values and derived values for the considered attributes.

	Between channels	Within channel
Voltage	±1.70 mV	±0.05 mV
Current	±5.20 mA	±2.28 mA
Temperature	±0.1 °C	±0.1 °C
Capacity	≤±20.8 mAh	≤±9.1 mAh
Pulse Resistance	≤±0.31% R_p	≤±0.12% R_p
Impedance	±1%|Z| ± 1°	±1%|Z| ± 1°

amplification cannot occur. The ambient temperature has a slight temperature gradient within the temperature chamber, but the average cell temperature increases about 5 °C during cycling and the temperature distribution widens as well (see Fig. 5). This indicates, that the differences in energy efficiencies (and thus losses) of the cells have more impact than the ambient temperature.

The BOL tests were conducted in a separate temperature chamber with four electrical circuits. Due to a lower temperature gradient and less variance in the measurement values for these four circuits, the uncertainties in the initial attributes tend to be even lower. Then the cycling and RPT were conducted on one circuit per cell, the assignment was not changed during the experiment.

3. Experimental results

The different aging trends of all 48 cells are shown in Fig. 6. The crosses mark the values taken from the capacity tests during BOL (first cross) and RPT (all others). The solid line is a smoothed cubic spline used for interpolation. This interpolation method is used because a linear interpolation would lead to sudden changes in the degradation rate which are not plausible. Two possible end of life (EOL) criteria are indicated by the dashed lines: the point where the cells reach an actual capacity of 1.55 Ah (84% of the average initial capacity) and 1.2 Ah (65%). These points were chosen instead of the standard 80% limit because these two points lie within the nearly linear zones of the two aging mechanisms. The choice of an interpolation function therefore has low impact on the calculated lifetimes used for the dependency analysis.

One can clearly distinguish between two aging mechanisms with different degradation rates. At first only a slow and nearly linear degradation mechanism is present, after about 1000 cycles a second mechanism starts to occur, with a much higher degradation rate. The same characteristics are seen in Dubarry et al. ([14], Fig. 10) and are assigned to lithium loss in the first part and active material loss in the second part by using incremental capacity analysis.

The capacity variance and therefore the cycle lifetime of the different cells is significantly spreading over the course of the experiment. Different degradation rates seem to increase the spreading in the first part of the aging cycles. But even the turning point where the second mechanism gains influence is not constant, causing much higher variance. After the transition the new degradation rates are quite similar. One would expect that the cell with the highest initial degradation rate also ends up as the worst performing cell in later phases of the experiment. But this is not the case. In Fig. 7 the position of the different cells after sorting from

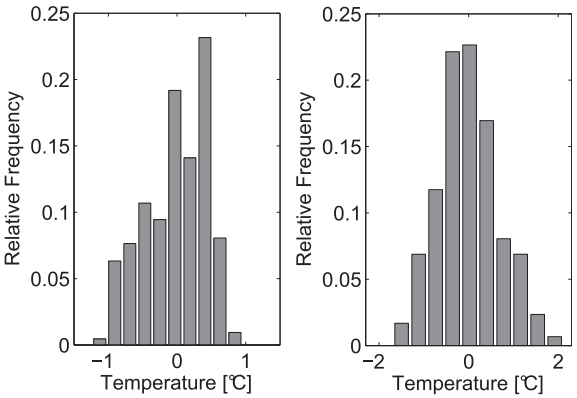

Fig. 5. Ambient temperature distribution (left) and cell temperature distribution during cycling (right).

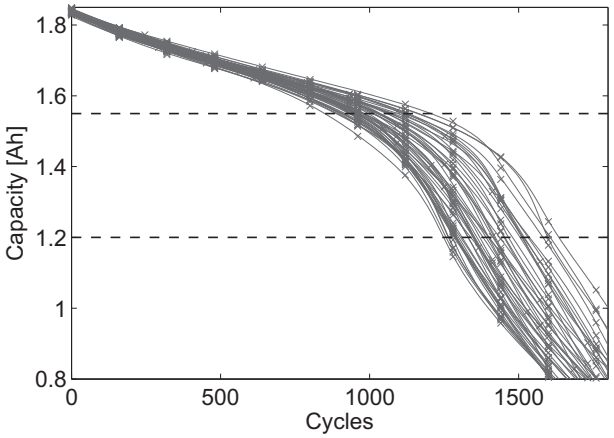

Fig. 6. Different aging trends from 48 equal cells under same aging conditions and profiles.

lowest to highest capacity after different cycle lifetimes can be seen. A cell that is in the lower third of the capacities after 480 cycles can end in the top ten cells after 1440 cycles (see highlighted line) due to different transition points and degradation rates.

Initially there is only a slight difference between the maximum and minimum capacity (denoted by capacity spread) as seen in Fig. 8. Up to 600 cycles the spread increases slowly. Then a faster increase starts and after 1500 cycles the spread is nearly constant. This behavior can be explained by the different aging mechanism and transition points into the second aging mechanism. One would think that everything is fine if a battery pack is designed to stay within the first part where the aging speed and capacity spread is low. But one has to consider, that the average aging slope in the first part is only one quarter as steep as in the second part. This can be seen if the difference between the maximum and minimum cycle life at a given EOL capacity is focused (see Fig. 9). Even the very low initial capacity spread causes considerable differences in the cycle lifetimes for very high EOL capacities. At 1.5 Ah (about 80% of the initial capacity) the cycle lifetime spread already reaches its maximum value and stays nearly constant. Consequently the slope of the aging effect has a large influence on the impact of aging differences. The more even the slope, the greater the amplification of aging differences is.

It can be summarized that there is a considerable capacity spread during aging even under equal conditions. This spread has to be considered during battery pack design and manufacturing. As

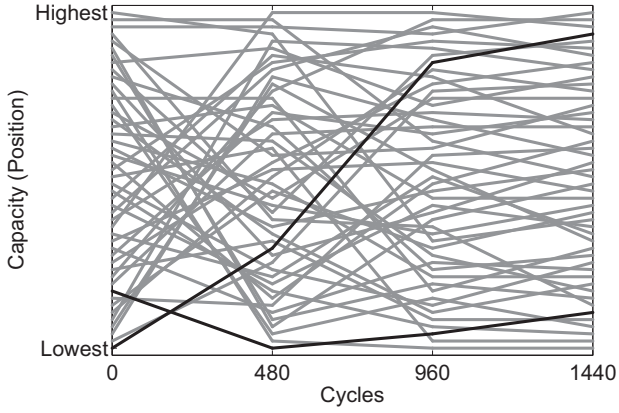

Fig. 7. Development of the position of the 48 cells within the sorted capacity at four cycle lifetimes.

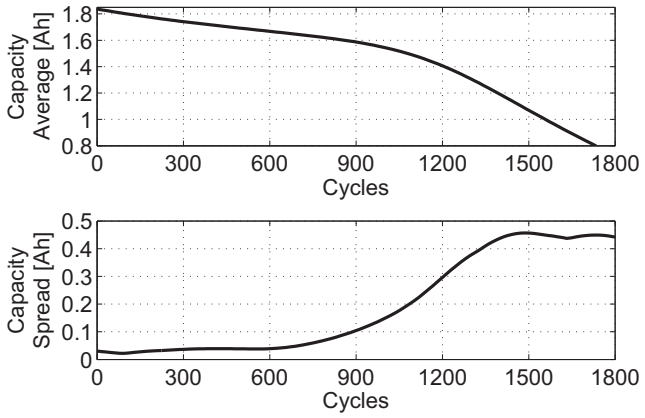

Fig. 8. Average capacity and capacity spread after different number of cycles.

the lithium-ion cells get better in their cycle lifetime, care has to be taken that the aging variance improves on the same scale. Else the amplification mechanism and the limitation by the weakest cell can completely defeat the improvement. If there is no possibility to access the production process, a classification into different batches based on a predicted cycle lifetime could lead to reduced variance.

4. Dependency analysis

As the different aging mechanism in lithium-ion batteries itself are hardly understood until now, there is no theory known on how the aging behavior can be deduced from attributes that can be measured initially (at begin-of-life). Therefore a broad approach is used in this chapter. All available attributes are investigated by statistical methods and data mining algorithms to attain an empirical model and get some insights on the most significant attributes.

For the dependency analysis the two end of life criteria (84% and 65%, given in Chapter 3) are used to calculate the cycle lifetimes. With this choice the influence of the used interpolation function is as small as possible and differences in the dependencies can be identified more reliable.

Table 3 lists the attributes with a correlation factor greater than 0.5 with the cycle lifetime for the 84% criterion. The correlations are significant according to the Student's *t*-distribution with 46 degrees of freedom [15], but a good prediction is hardly possible with one of these values as can be seen in Fig. 10. The use of multiple linear

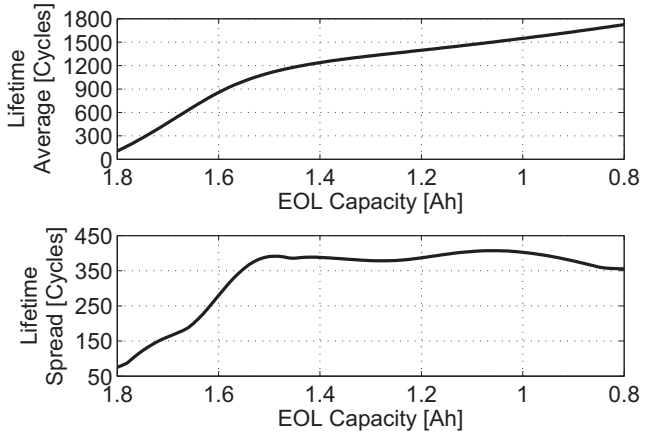

Fig. 9. Average lifetime and lifetime spread for different EOL criteria.

Table 3
The four attributes most correlated to the cycle lifetime for the 84% criterion.

Attribute	Correlation	Label in Fig. 10
Real part of the local minimum impedance at 70% SoC and 0 °C	0.595	Attr. 1
Frequency of the local minimum impedance at 70% SoC and 25 °C	0.566	Attr. 2
Imaginary part of the local minimum impedance at 50% SoC and 25 °C	0.521	Attr. 3
Pulse resistance at 70% SoC, 0 °C, 6 A discharge, 15 s	0.512	Attr. 4

regression promises to combine different attributes and their correlation to get a better prediction.

Prediction. Since the possibility for errors increases as the number of attributes and thus the complexity rises, a number of preprocessing steps were applied to the dataset. With a visual inspection values with measurement errors were removed (one capacity test). About 20 pulse resistance values were missing due to recording errors. Since only one or two values within a set were missing, these were replaced with the mean value of the example set to be able to still use the attribute for prediction. All attributes with a standard deviation less than the standard uncertainty of the measurement (given in Chapter 2) were also removed from the dataset. These do only contain measurement noise and cannot contribute to the prediction accuracy especially if the model is used to predict untrained examples. Starting with 950 attributes, the step removed many attributes with temperature measurements and all capacity measurements due to low deviations, resulting in 630 valid attributes. From attribute pairs with a correlation greater than 0.95 only one was kept, because all others do not add any new information and can only cause misleading attribute selections. Many pulse resistances with similar time constants were removed by this step. The 385 attributes that were identified to be significant are considered for further analysis.

Due to the much larger amount of attributes than measured examples care has to be taken to prevent overfitting. Therefore the maximum number of attributes used for the linear regression was limited to 24. Via forward selection the best attribute selection was determined. To measure the performance of different selections a cross-validation scheme was used, reducing the probability for overfitting furthermore. The linear regression model was trained with all but one example which was then predicted with this model. The mean absolute error from all validations was used to

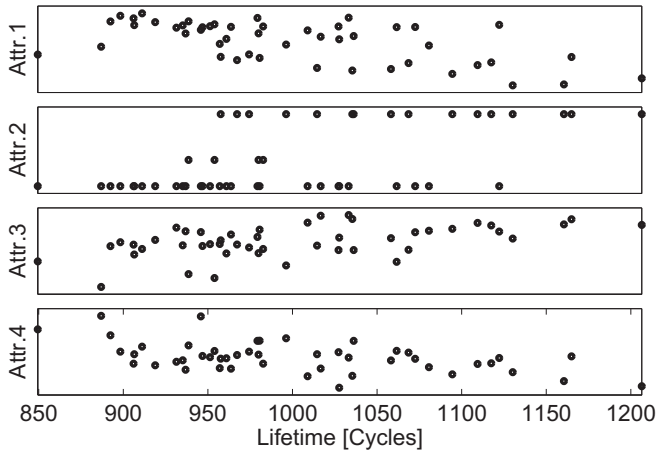

Fig. 10. Graphical representation of the correlation. The calculated lifetime and value of the four attributes given in Table 3 are plotted for each of the 48 cells.

Table 4
Performance measures of the linear regression for both end-of-life criteria and four different selections of attributes.

	Valid. error [cycles]	Model error [cycles]	R^2	Attributes
EOL @ 84%				
All attributes	16.35	8.15	0.97	24
Attr. @ 25 °C	26.49	13.22	0.94	24
25 °C, 30% SoC	46.11	32.98	0.67	13
Uncond. attr.	58.29	37.03	0.59	17
EOL @ 65%				
All attributes	22.57	13.79	0.94	19
Attr. @ 25 °C	31.92	15.31	0.97	24
25 °C, 30% SoC	60.69	32.45	0.83	22
Uncond. attr.	66.09	50.36	0.49	10

guide the attribute selection. With the resulting selection the final model was then trained. All steps were calculated within the RapidMiner data mining environment [16].

The goal for a classification based on the predicted lifetime in a production line is to have a measurement procedure with a duration as low as possible. To account for this need the regression model was computed with four different sets of attributes. With all available attributes, only including the attributes measured at 25 °C, only including the attributes measured at 25 °C and 30% SoC, which is near to the delivery SoC and only with the attributes measured without any preconditioning. The results for both end of life criteria can be found in Table 4. Given is the mean absolute error during cross validation, the mean absolute error from the final model together with the coefficient of determination and the number of attributes that were selected during forward selection. The overall range of measured cycle lifetimes for the 84% criterion is 350 cycles (from 850 to 1200) and 400 cycles (from 1250 to 1650) for the 65% criterion.

The performance results of the models with the unconditioned attributes and with the attributes at low SoC are not satisfying. A classification based on these predictions would lead to a failure rate which is too high. But both other models do perform quite well (although the model with the 65% end of life criterion and all attributes seems to get stuck in a local minimum). The models with the 25 °C attributes give the best compromise between prediction accuracy and measurement effort and thus are selected for further investigation. Fig. 11 does show one possible classification in two groups based on the prediction. A few examples would be classified

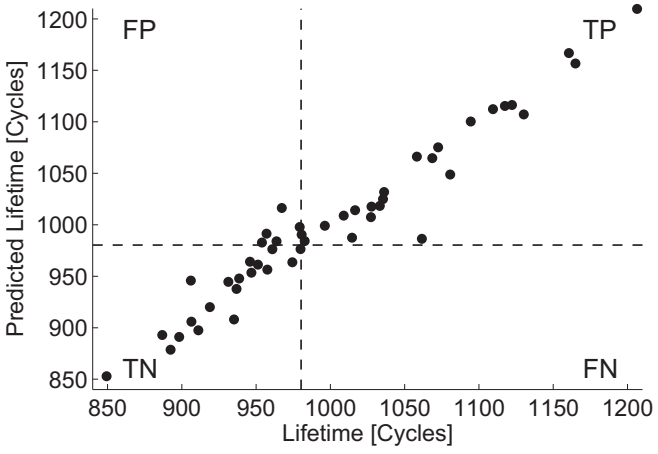

Fig. 11. Predicted and measured cycle life (for the 84% criterion). The lines indicate a possible classification above and below the median. A few false positive decisions would be made.

Table 5
Top ten attributes for the linear regression sorted by significance. All attributes measured at 25 °C.

EOL @ 84%	Sign
Imaginary part of the local minimum impedance at 30% SoC	+
Pulse resistance at 30% SoC, 6 A discharge, 20 s	−
Frequency of the zero crossing at 50% SoC	+
Frequency of the local minimum impedance at 70% SoC	+
Pulse resistance at 50% SoC, 4A charge, 15 s	−
Frequency of the local maximum impedance at 70% SoC	+
Pulse resistance at 30% SoC, 6 A discharge, 2 s	+
Pulse resistance at 50% SoC, 6 A discharge, 1 s	−
Pulse resistance at 30% SoC, 2 A charge, 2 s	−
Pulse resistance at 30% SoC, 4 A charge, 0.4 s	+
EOL @ 65%	**Sign**
Pulse resistance at 50% SoC, 4 A charge, 15 s	−
Pulse resistance at 50% SoC, 4 A charge, 20 s	+
Pulse resistance at 30% SoC, 2 A charge, 5 s	+
Pulse resistance at 70% SoC, 4 A charge, 10 s	−
Pulse resistance at 50% SoC, 4 A discharge, 1 s	+
Pulse resistance at 30% SoC, 6 A discharge, 2 s	+
Pulse resistance at 70% SoC, 2 A charge, 0.4 s	+
Pulse resistance at 50% SoC, 4 A discharge, 2 s	−
Pulse resistance at 50% SoC, 6 A discharge, 1 s	−
Pulse resistance at 50% SoC, 4 A charge, 2 sc	−

as belonging to the wrong group, but the measured lifetime differs only slightly from the chosen threshold. This indicates that a good prediction of the cycle lifetime is possible with these models at least for this experiment.

The most significant attributes that were chosen for the two prediction models are shown in Table 5 (sorted by significance level, common attributes in bold). If there was a clear cause for the different aging trends there should be some clusters of similar attributes. But the lists are completely mixed: high and low time constants, high and low current rates and all used SoC levels are present. Comparing the two end of life criteria there are only three common attributes. The variation of the two aging mechanisms therefore also seems to be caused by different effects and therefore represented by different attributes.

5. Discussion

The experiment was setup to minimize the differences in operating conditions, measurement uncertainty and cell variance. It was shown by verification measurements that this requirement was held. However the capacity trend shows a significant spread in the different aging trends which therefore has to be accounted for cell production based variances. The differences in cycle lifetime have to be considered in battery pack design or have to be reduced by cell selection.

By using a linear regression model it is possible to predict the lifetimes measured in this experiment. The correlations between multiple attributes and the expected lifetime are used for this purpose. It is not yet verified if the selected attributes are also sufficient to predict the trend under other operating conditions like temperature or cycle depth, or if the aging trend variance depends on these conditions, too. Even more, the same experiment should be repeated with a calendar aging procedure to quantify the variance of the aging mechanisms occurring in this case.

The most significant attributes in the regression do not allow drawing clear conclusions between causes and the observed effects. Maybe other attributes, which are more closely related to electrochemical parameters have to be included to get a better possibility to identify contributing causes. Likewise a larger sample base (e.g. field data) would be desirable, but usually there is no

comprehensive test data of cells used in battery pack production. Lifetime data from field tests, if available, is usually not broken down to cell level and furthermore influenced by the battery pack design and usage profiles.

Because of the empirical nature of the given dependency analysis the results are not per se transferable to other cells or applications. Therefore besides further investigation other measures have to be taken to reduce the effect of different aging trends. For example a parallel connection of multiple smaller cells can be beneficial, because the different aging trends are averaged.

6. Conclusion

Even in mass production lines for lithium-ion batteries there are variances of material properties and process parameters which lead to different behavior of the individual cells. It was experimentally proven that these variances affect the aging behavior too. The worst cell showed a cycle lifetime just three quarters as high as the cycle lifetime of the best cell. Parameter have been identified which can be measured at begin-of-life and allow predicting the aging behavior. Further investigations have to be conducted to verify that theses dependencies hold under varying operating conditions as well.

Acknowledgments

This work was sponsored by the German Federal Ministry of Education and Research (BMBF) under contract no. 13N12035 as part of the project “eProduction” [17].

References

[1] S. Santhanagopalan, R.E. White, Int. J. Electrochem. (2012), http://dx.doi.org/10.1155/2012/395838.
[2] P. Arora, R.E. White, M. Doyle, J. Electrochem. Soc. 145 (10) (1998) 3647–3667, http://dx.doi.org/10.1149/1.1838857.
[3] M. Ecker, J.B. Gerschler, J. Vogel, S. Käbitz, F. Hust, P. Dechent, D.U. Sauer, J. Power Sources. ISSN: 0378-7753 215 (0) (2012) 248–257, http://dx.doi.org/10.1016/j.jpowsour.2012.05.012.
[4] S. Käbitz, J.B. Gerschler, M. Ecker, Y. Yurdagel, B. Emmermacher, D. André, T. Mitsch, D.U. Sauer, J. Power Sources. ISSN: 0378-7753 239 (2013) 572–583, http://dx.doi.org/10.1016/j.jpowsour.2013.03.045.
[5] Y. Zhang, C.-Y. Wang, J. Electrochem. Soc. 156 (7) (2009) A527–A535, http://dx.doi.org/10.1149/1.3126385.
[6] R. Wright, C. Motloch, J. Belt, J. Christophersen, C. Ho, R. Richardson, I. Bloom, S. Jones, V. Battaglia, G. Henriksen, T. Unkelhaeuser, D. Ingersoll, H. Case, S. Rogers, R. Sutula, J. Power Sources. ISSN: 0378-7753 110 (2) (2002) 445–470, http://dx.doi.org/10.1016/S0378-7753(02)00210-0.
[7] W. Prochazka, G. Pregartner, M. Cifrain, J. Electrochem. Soc. 160 (8) (2013) A1039–A1051, http://dx.doi.org/10.1149/2.003308jes.
[8] M. Dubarry, C. Truchot, M. Cugnet, B.Y. Liaw, K. Gering, S. Sazhin, D. Jamison, C. Michelbacher, J. Power Sources. ISSN: 0378-7753 196 (23) (2011) 10328–10335, http://dx.doi.org/10.1016/j.jpowsour.2011.08.077.
[9] E. Thomas, I. Bloom, J. Christophersen, V. Battaglia, J. Power Sources. ISSN: 0378-7753 184 (1) (2008) 312–317, http://dx.doi.org/10.1016/j.jpowsour.2008.06.017.
[10] M. Dubarry, N. Vuillaume, B.Y. Liaw, J. Power Sources. ISSN: 0378-7753 186 (2) (2009) 500–507, http://dx.doi.org/10.1016/j.jpowsour.2008.10.051.
[11] S. Paul, C. Diegelmann, H. Kabza, W. Tillmetz, J. Power Sources. ISSN: 0378-7753 239 (2013) 642–650.
[12] W.-C. Lih, J.-H. Yen, F.-H. Shieh, Y.-M. Liao, in: 2012 International Symposium on Computer, Consumer and Control (IS3C), 2012, pp. 381–384, http://dx.doi.org/10.1109/IS3C.2012.103.
[13] Joint Committee for Guides in Metrology, JCGM 100: Evaluation of Measurement Data – Guide to the Expression of Uncertainty in Measurement, BIPM, 2008.
[14] M. Dubarry, C. Truchot, B.Y. Liaw, K. Gering, S. Sazhin, D. Jamison, C. Michelbacher, J. Power Sources. ISSN: 0378-7753 196 (23) (2011) 10336–10343, http://dx.doi.org/10.1016/j.jpowsour.2011.08.078.
[15] H. Rinne, Taschenbuch der Statistik, fourth ed., Wissenschaftlicher Verlag Harri Deutsch GmbH, Frankfurt am Main, 2008, ISBN 978-3-8171-1827-4.
[16] I. Mierswa, M. Wurst, R. Klinkenberg, M. Scholz, T. Euler, in: L. Ungar, M. Craven, D. Gunopulos, T. Eliassi-Rad (Eds.), KDD'06: Proceedings of the 12th ACM SIGKDD International Conference on Knowledge Discovery and Data Mining, ACM, New York, NY, USA, 2006, ISBN 1-59593-339-5, pp. 935–940, http://dx.doi.org/10.1145/1150402.1150531.
[17] URL, http://www.audi.de/eprod/brand/de.html, 2013.